

CrossMark
click for updates

Three distinct open-pore morphologies from a single particle-filled polymer blend†

Trystan Domenech, Junyi Yang, Samantha Heidlebaugh and Sachin S. Velankar*

Cite this: *Phys. Chem. Chem. Phys.*,
2016, 18, 4310Received 8th December 2015,
Accepted 11th January 2016

DOI: 10.1039/c5cp07576a

www.rsc.org/pccp

Ternary mixtures composed of polyisobutylene (PIB), polyethylene oxide (PEO), and silica particles yield three distinct open-pore morphologies depending on the mixture composition: (1) pendular network (particles bonded together by menisci of PEO); (2) capillary aggregate network (particles and PEO form a combined phase with strongly solid-like properties which forms a percolating network); (3) cocontinuous morphology (silica and the PEO form a highly viscous combined phase which retards interfacial tension-driven coarsening). Remarkably, interfacial tension plays altogether different roles in stabilizing these three morphologies: stabilizing the first, not affecting the second, and destabilizing the last. The first two of these morphologies appear to be generalizable to other systems, e.g. to oil/water/particle mixtures. In all three cases, the pores do not collapse even after flow, i.e. all three porous morphologies are amenable to processing.

Introduction

Open pore structures are useful in a wide variety of applications, e.g. absorbing and retaining fluids (e.g. wound dressing, personal hygiene, oil spill absorption), highly compliant structures (e.g. seat cushions), and providing percolating pathways (conductive electrodes, battery separator materials, filters, tissue engineering scaffolds). Topologically, open pore structures have two interpenetrating continuous phases, one of which is regarded as “porous” (i.e. typically filled with air or with water), and the other phase being a solid with some mechanical integrity. Open pore structures have diverse morphologies such as networks composed of slim struts (e.g. open cell foams¹), interconnected cavities (e.g. polymerized high-internal phase emulsions^{2–5}), interstitial spaces between fused particles (e.g. sintered powders⁶) or between fiber mats,^{7,8} or smooth bicontinuous phases.^{9,10} Here we show that a single system composed of two immiscible

polymers and one particulate species yields three distinct open-pore morphologies depending on the composition of the mixture.

Experimental

The experimental system is composed of silica particles and two immiscible polymers, polyethylene oxide (PEO) and polyisobutylene (PIB). Details of the materials are provided in Table 1. All components were mixed together (next paragraph) at 80 °C, a temperature at which the PEO and PIB have similar viscosities. Upon cooling to room temperature, the PEO crystallizes into a semicrystalline solid (melting point ~65 °C); this provides a facile means of quenching the morphology developed under melt-blending conditions. The continuous-phase PIB was extracted in octane, leaving behind the consolidated masses of the PEO and the particles discussed below. These were fractured, coated with palladium, and imaged by scanning electron microscopy (SEM).

Being composed of molten polymers, these samples have viscosities far higher than oil/water mixtures. Accordingly they cannot be mixed by simple shaking or by using equipment such as a homogenizer. Therefore, the samples were mixed in a custom-built polymer mixer comprising a rotating disc-cup assembly of 5 ml volume. Three ball bearings were added between the rotating disc and the cup to ensure intensive mixing.^{11–13} The cup was maintained at 80 °C using an electric heater. All samples were mixed identically: the minority polymer PEO was first dispersed into the PIB at 1200 rpm, particles were added, and the mixing was continued for an additional 5 min. The samples were cooled in air immediately after mixing, followed by holding for 30 minutes at ~4 °C to ensure complete crystallization of the PEO.

Results and discussion

The six different compositions discussed in this article can be placed in a ternary composition diagram,^{14,15} Fig. S1 (ESI†),

Department of Chemical Engineering, University of Pittsburgh, Pittsburgh, PA 15261, USA. E-mail: velankar@pitt.edu; Tel: +1-412-624-9984

† Electronic supplementary information (ESI) available. See DOI: 10.1039/c5cp07576a

Table 1 Properties of the materials used

	Viscosity (80 °C)	M_w	Supplier
Polyethylene oxide (PEO)	13 Pa s	20 kg mol ⁻¹	Fluka
Polyisobutylene (PIB)	8 Pa s	2400 g mol ⁻¹	Soltex
Silica average $\sim 2 \mu\text{m}$ diameter			Industrial powder

from which the volume fractions of all three species can be read off. However, for this article, it is more convenient to specify the composition in terms of two parameters: the particle volume fraction, ϕ_p , and $\varrho = \phi_{\text{PEO}}/\phi_p$, which is the wetting fluid loading relative to the particle loading. This representation is shown in Fig. 1A. Of the six compositions discussed, the three with high values of ϕ_p yield three distinct types of open-pore structures illustrated schematically in Fig. 1B, and discussed below.

Fig. 2A illustrates the first kind of porous structure, dubbed a pendular network. This appears when the PEO loading is substantially lower than particle loading, *i.e.* ϱ is on the order of 0.1, and no larger than 0.3. In this range of ϱ , when the sample is well mixed, the wetting fluid forms pendular menisci that connect the particles to form aggregates. If ϕ_p is small, the pendular aggregates are discrete (Fig. S2, ESI[†]). With increasing ϕ_p (at fixed ϱ), these aggregates grow until they percolate, and a pendular network results. Previously we showed that the percolation threshold is only a few percent,¹² *i.e.* the ϕ_p of Fig. 2A far exceeds the percolation threshold. This pendular network structure is analogous to the wet sand in which the sand particles are bridged by menisci of water.¹⁶

Fig. 2B illustrates the second kind of porous structure dubbed a capillary aggregate network, which appears when ϱ

is 0.5–1. Since the particles are fully wetted by the PEO, and since the PEO fraction is comparable to the particle fraction, the PEO engulfs the particles completely to form a combined phase. This combined phase is highly concentrated with an internal particle volume fraction of $\phi_p^{\text{combined}} = \frac{\phi_p}{\phi_p + \phi_{\text{PEO}}} = (1 + \varrho)^{-1}$. The dependence of ϕ_p^{combined} on ϱ is illustrated in Fig. 3A. For instance, for Fig. 2B, $\varrho = 0.9$, which corresponds to $\phi_p^{\text{combined}} = 0.53$. Due to this high particle loading, this combined phase is expected to resemble a paste with solid-like rheological properties. We sought to measure the rheology directly by preparing a particle-in-PEO suspension (no PIB added) at a particle loading of 53 vol%. However, we were unsuccessful since the extremely solid-like rheology makes homogeneous mixing difficult. We were however able to prepare particle-in-PEO suspensions with somewhat lower particle loadings and Fig. S4 (ESI[†]) shows the Large Amplitude Oscillatory Shear (LAOS) rheology of some samples measured at a frequency of 10 rad s⁻¹. At 40 vol% particles, G'' exceeds G' over the entire amplitude range, indicative of a liquid-like behavior. In contrast, at 44 and 50% particles, the rheological behavior is typical of paste-like materials: at low amplitude, $G' > G''$, whereas at some larger amplitude, there is a crossover which is often regarded as a signature of yielding. From these data, one may extract the linear viscoelastic moduli of these suspensions (Fig. 3B), and by interpolation, conclude that samples with over $\sim 42\%$ particles have $G' > G''$, indicative of solid-like rheology. Thus, a suspension with 53% particles (corresponding to the PEO-phase in Fig. 2B) would be strongly solid-like. Accordingly, when the ternary blend of Fig. 2B is subjected to intense mixing, the combined phase tends to form misshapen “blobs” called capillary aggregates.¹⁷ Capillary aggregates tend to be non-spherical since their internal yield stress exceeds their capillary pressure, thus interfacial tension cannot induce a misshapen aggregate to relax into a spherical shape. At low values of ϕ_p these blobs are discrete (Fig. S3, ESI[†]); however, with increasing ϕ_p , they percolate into the network of Fig. 2B. This network is composed of roughly spherical capillary aggregates which are bonded together through relatively narrow necks.¹² This phenomenon has been documented previously in mixtures of oil, water, and fat where it was called partial coalescence.¹⁸ A more evocative term coined by Caggioni *et al.* is anisotropic endoskeletal drops,¹⁹ *i.e.* drops with an internal network that sustains non-spherical shapes. We note that the particles in these previous papers were needle-like crystals,^{18,19} and hence could develop a yield stress at even low particle loadings. Here, the particles are spherical, and hence anisotropic drop shapes can survive only at high ϕ_p^{combined} (low ϱ) values. Incidentally, the fact that capillary aggregates are formed at certain compositions is not new;¹⁷ what is unusual is that the capillary aggregates join together into a percolating network.

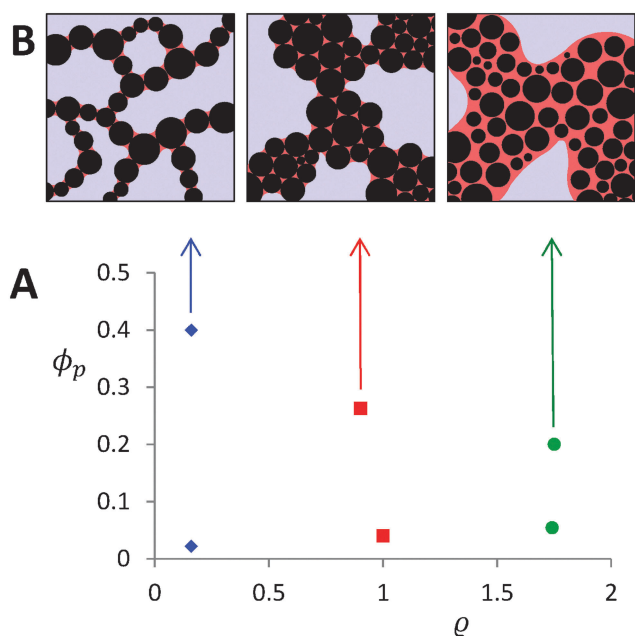


Fig. 1 (A) Compositions of the samples discussed in the article. The same compositions are represented within a ternary composition diagram in Fig. S1 (ESI[†]). (B) Idealized illustrations of the three different types of porous structures corresponding to the compositions indicated by the arrows.

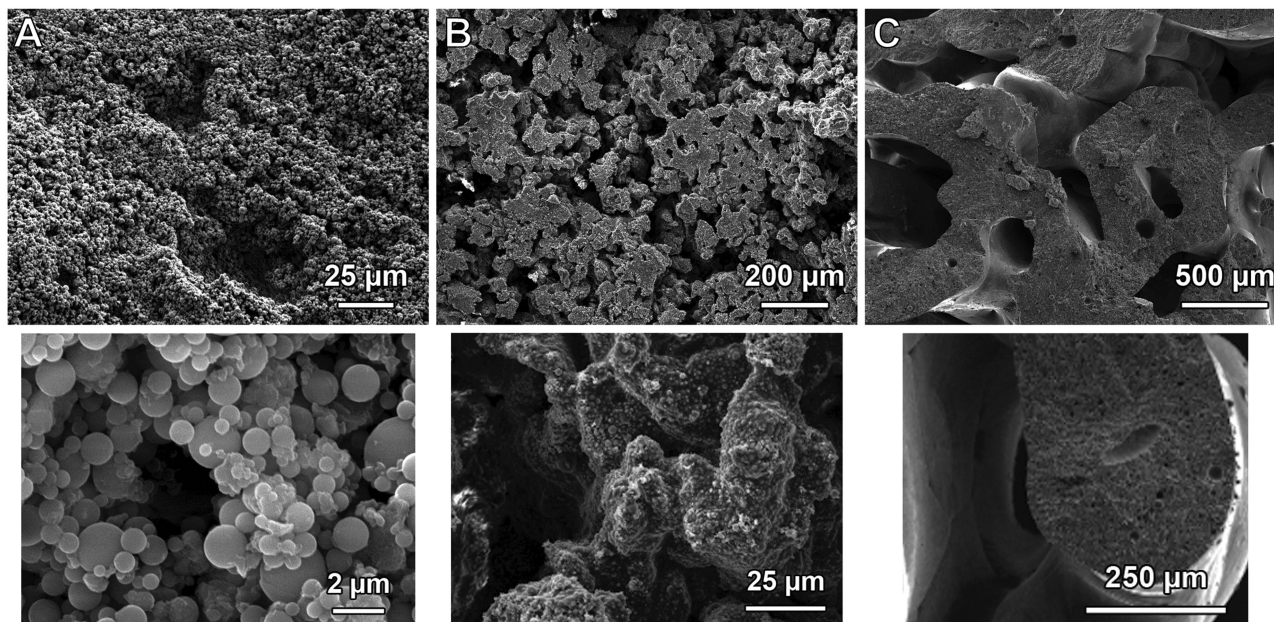


Fig. 2 (A) Pendular network; (B) capillary aggregate network; and (C) cocontinuous morphology. Images in the lower row are the same samples as the upper row, but at a higher magnification.

The third type of porous structure, dubbed a cocontinuous morphology (Fig. 2C), is evident at $\varrho = 1.75$. The particles and the PEO still form a combined phase, but now the combined phase is much less crowded than that in Fig. 2B. For example, for Fig. 2C for which $\varrho = 1.75$, the particle volume fraction in the combined phase is 0.36 (Fig. 3A). At this particle loading, the combined phase is highly viscous, but it no longer has significant solid-like properties (indeed even at 40% particles, Fig. S4, ESI,† indicates liquid-like rheology). Accordingly, particles no longer protrude out from the PEO phase; instead the liquid/liquid interface appears smooth, as typical of systems in which capillarity dominates. Under these conditions, if the combined phase is dilute (Fig. S5, ESI†), the morphology is composed of spherical drops of PEO with particles incorporated inside. In Fig. 2C in contrast, the combined phase loading is $(\phi_p + \phi_{\text{PEO}}) = 0.55$, and a cocontinuous morphology is obtained. Given sufficient time under quiescent conditions after mixing, this system would coarsen indefinitely, and eventually the cocontinuous structure would be destroyed by gravity (there is a significant density difference between the phases due to the high density of silica). Yet, due to the high internal viscosity of the combined phase, coarsening and collapse are relatively slow processes. Thus even air-cooling is sufficiently rapid that the crystallization of PEO can quench the cocontinuous structure readily. It is crucial to note that the particle-free PEO/PIB blends do not form cocontinuous morphologies at any PEO:PIB ratio. We have prepared particle-free PEO/PIB blends across a range of compositions and in all cases; the morphology is either a PEO-in-PIB with spherical PEO drops, or *vice versa*.²⁰ Thus, the particles are essential to stabilize the cocontinuous morphology. We surmise that the mechanism for such stabilization resembles viscoelastic phase separation:²¹ since the combined PEO + particles phase

has a high viscosity, interfacial coarsening and breakup, which usually destroy a cocontinuous morphology, are greatly retarded. Incidentally, we note that cocontinuous morphologies are commonly reported in the polymer blends literature, even in the absence of particles.⁹ In those cases, the polymers being blended have viscosities that are typically 2–3 orders of magnitude higher than those used here. Due to those high viscosities, the morphologies can be quenched readily by cooling.

It is important to note explicitly the major differences between the three morphologies. The pendular network is inherently a particle-scale structure, with the capillary force playing the role of pair-wise attraction between particles. The percolating network is built from the individual particles bonded together by capillary menisci.¹⁶ The immediate implication is that the pore size is comparable to the particle size, *i.e.* as long as the network is homogeneous, the pore size can be changed only by changing the particle size. In contrast, the capillary aggregate network uses as building blocks not individual particles, but also aggregates comprising a large number of particles together engulfed by the wetting fluid. Thus, the pore size is decoupled from the particle size, and is instead set by the composition (which determines the rheology of the combined particle + PEO phase) and by the mixing conditions (which determine the size of the largest capillary aggregate that can survive the mixing process). Finally the pore size of cocontinuous morphology is also decoupled from the particle size. But unlike in capillary aggregates, the combined phase is not internally jammed, and its rheological behavior is liquid-like. Thus, this morphology is unstable, and unlike the previous two morphologies, quenching is essential to suppress morphological coarsening. In the present case, quenching is accomplished by the crystallization of PEO, but one may also arrest coarsening by gelation, vitrification,

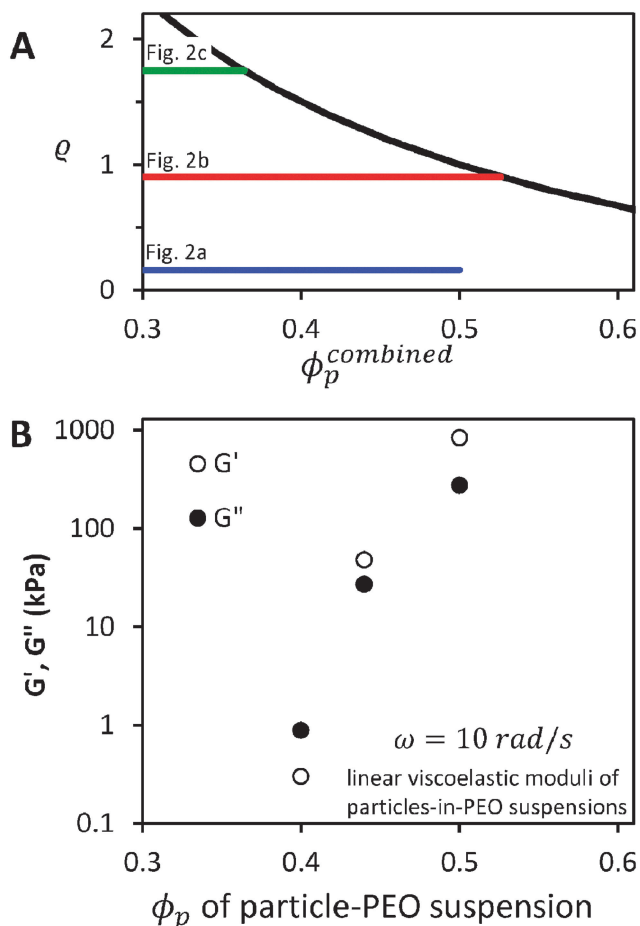


Fig. 3 (A) The function $\phi_p^{\text{combined}} = (1 + \rho)^{-1}$, corresponding to the particle volume fraction in the PEO-phase of a PIB/PEO/particle blend. The three horizontal lines correspond to the ρ values of the three porous structures of Fig. 2. (B) Linear viscoelastic moduli G' and G'' of suspensions of particles in PEO.

or crosslinking of one or both phases. Since the cocontinuous morphology results from a competition between viscous stress and interfacial tension, we anticipate that the size-scale of the morphology would reduce if the mixing speed were to be increased, although we have not tested this.

It is interesting to note that capillarity (in the sense of minimizing the liquid–liquid interfacial area) plays completely different – indeed opposing – roles in these three cases. In the pendular network, the pairwise attractive force between the particles is attributable to interfacial tension (indeed the meniscus force is proportional to the interfacial tension).²² Thus the stability of the particle network depends primarily on capillarity; any additional interparticle attractions would confer additional stability. In contrast, the capillary aggregate network is stabilized primarily by the solid-like rheology of the combined particle + PEO phase, and to a first approximation, the stability does not rely on capillarity. In a previous article on oil/water/particle systems,¹⁵ we have argued that since particles protrude out of the surface of the capillary aggregates, the liquid/liquid interface has a negative curvature, and hence “pulls together” the particles

with a Laplace pressure that is on the order of (surface tension)/(particle size). This Laplace pressure increases the interparticle friction forces, and may therefore increase the yield stress within the capillary aggregates. To the extent that this mechanism is active, capillarity may have a stabilizing effect on the capillary aggregate network. Finally, in the cocontinuous morphology, capillarity induces morphological coarsening as well as breakup into a droplet-matrix morphology. Thus, in this case, capillarity has a destabilizing effect. It is for this reason that the cocontinuous structure must be quenched, whereas the pendular or capillary aggregate networks need not be.

It is of immediate interest to ask whether these three morphologies are unique to polymeric mixtures, or if they may be realized even when the fluids are oil and water. The pendular network is highly general and can be realized in almost any particulate system in which the particles are preferentially wetted by the minority phase. For instance, Fig. S6 (ESI[†]) illustrates a pendular network realized from large glass particles, but using oil as the continuous phase and water as the dispersed phase that forms the meniscus. With hydrophobic particles, one may also realize an inverted structure in which water is continuous and oil is the meniscus-forming phase. The capillary aggregate network also appears to be generalizable to oil/water systems. For instance, Fig. S7A and B (ESI[†]) show a network formed by using the same particles as used in the rest of this paper, but with oil and water as the two fluids. The sample was mixed using a high speed rotor–stator mixer following the procedure described in the caption of Fig. S7 (ESI[†]). A network of capillary aggregates is clearly evident at $\rho = 0.75$. The same procedure was applied using polyethylene particles, methanol and a small quantity of mineral oil (see the caption of Fig. S8, ESI[†] for compositions). Since the polyethylene particles are highly oleophilic, a capillary aggregate network with methanol as the continuous phase was realized. Finally, we were unsuccessful in realizing cocontinuous morphologies from oil/water systems. For instance, Fig. S7A and B (ESI[†]) show capillary aggregates realized in an oil/water system at $\rho = 0.75$. Upon increasing the ρ to 0.8, the capillary aggregates become capable of complete coalescence, indicative of increasingly liquid-like behavior of the (silica + water) combined phase. But instead of realizing a cocontinuous morphology, Fig. S7C (ESI[†]) shows that the system collapses into a separated mixture of oil and (silica + water). Thus even if the cocontinuous morphology was present during mixing, it does not survive for any significant duration after mixing. We believe that this rapid collapse is attributable to the much lower fluid viscosity of the oil/water system as compared to the PEO/PIB blends. Thus, as already emphasized above, the cocontinuous morphology can be realized only if at least one of the fluid phases can be solidified rapidly. In summary, at least two of the three morphologies appear to be generalizable to oil/water systems; whereas the last, the cocontinuous structure, is not.

We have not investigated in detail the boundaries separating these three porous structures. A review across a wide range of systems suggests that the pendular aggregate morphology becomes unstable when menisci binding different particles start coalescing together.¹⁴ This happens at $\rho \sim 0.35\text{--}0.5$, which may be taken as

the boundary separating a pendular network from the capillary aggregate network. The boundary between capillary aggregates and cocontinuity (if cocontinuity is realized) depends on the ϱ value above which the combined phase has liquid-like rheology. This boundary is more difficult to generalize across a wide range of systems; depending on the nature of particle interactions, some combined phases may become solid-like at even relatively high ϱ values. Indeed, some previous researchers have reported the stabilization of cocontinuous-like morphologies in polymeric systems even at very low particle loading^{23–25} because the nanoparticles were able to induce solid-like rheology even at low particle loading.

Conclusions and outlook

In summary, we show that by changing the composition, a single three-component mixture yields three porous morphologies that have distinct size-scale and entirely different mechanisms of structural stabilization. What is most remarkable is that interfacial tension plays an altogether different role, stabilizing the pendular morphology, destabilizing the cocontinuous morphology, and (to a first approximation) not affecting the capillary aggregate network. At least two of these porous structures appear to be generalizable to other mixtures, including to oil/water/particle mixtures. Two noteworthy aspects that are relevant to practical applications must be emphasized. First, in all three of the porous structures reported here, both phases are continuous, *i.e.* they may be regarded as open-pore structures with potential applications listed in the first paragraph of this article. The resulting porous structures may be used directly, *e.g.* for tissue scaffolds. Alternately, one may remove the non-wetting fluid by selective extraction (as done here), drying, or simply draining out the fluid, and then undertake further modifications, *e.g.* particle sintering, back-filling the pores with other fluids, *etc.* Indeed particulate networks based on capillary attractions have already been used to fabricate porous ceramics.^{26,27} Second, all three of these structures were generated under flow conditions, and longer flow duration under molten conditions does not disrupt them. Thus, as long as the yield stress is not too high (which may happen at higher particle loadings), these morphologies are all amenable to be molded, extruded, or injected – without losing their open pore morphology. This is in contrast to many other methods of fabrication of similar open-cell porous structures, *e.g.* polymerization of high internal phase emulsion, preparation of a bijel precursor,¹⁰ leaching a porogen,²⁸ phase separation of a polymer solution, or direct foaming of polyurethanes. In all those cases, the open-celled porous structure cannot be subjected to flow, either because it is quenched or because it does not survive under flow.

Acknowledgements

We gratefully acknowledge the National Science Foundation for financial support (NSF-CBET grant no. 0932901 and 1336311), and Dr Manjulata Singh and Prof. Shilpa Sant for assistance

with confocal imaging (Fig. S6b, ESI[†]) respectively. Fig. S1 (ESI[†]) was drawn using the ternary diagram template provided by Graham and Midgley.²⁹

References

- 1 C. Defonseka, *Practical Guide to Flexible Polyurethane Foams*, Smithers Rapra Technology, 2013.
- 2 K. Haibach, A. Menner, R. Powell and A. Bismarck, Tailoring mechanical properties of highly porous polymer foams: Silica particle reinforced polymer foams *via* emulsion templating, *Polymer*, 2006, **47**(13), 4513–4519.
- 3 A. Barbetta, G. Rizzitelli, R. Bedini, R. Pecci and M. Dentini, Porous gelatin hydrogels by gas-in-liquid foam templating, *Soft Matter*, 2010, **6**(8), 1785–1792.
- 4 R. Foudazi, P. Gokun, D. L. Feke, S. J. Rowan and I. Manas-Zloczower, Chemorheology of Poly(high internal phase emulsions), *Macromolecules*, 2013, **46**(13), 5393–5396.
- 5 M. S. Silverstein, Emulsion-templated porous polymers: A retrospective perspective, *Polymer*, 2014, **55**(1), 304–320.
- 6 P. S. Liu and G. F. Chen, *Porous Materials: Processing and Applications*, Butterworth-Heinemann, Oxford, 2014.
- 7 R. Masoodi and K. Pillai, *Wicking in Porous Materials: Traditional and Modern Modeling Approaches*, CRC Press, Boca Raton, 2013.
- 8 B. Ding and J. Yu, *Electrospun Nanofibers for Energy and Environmental Applications*, Springer, Heidelberg, 2014.
- 9 P. Potschke and D. R. Paul, Formation of Co-continuous structures in melt-mixed immiscible polymer blends, *J. Macromol. Sci., Polym. Rev.*, 2003, **C43**(1), 87–141.
- 10 M. N. Lee and A. Mohraz, Bicontinuous Macroporous Materials from Bijel Templates, *Adv. Mater.*, 2010, **22**(43), 4836–4841.
- 11 M. Maric and C. W. Macosko, Improving polymer blend dispersions in mini-mixers, *Polym. Eng. Sci.*, 2001, **41**(1), 118–130.
- 12 T. Domenech and S. S. Velankar, On the rheology of pendular gels and morphological developments in paste-like ternary systems based on capillary attraction, *Soft Matter*, 2015, **11**(8), 1500–1516.
- 13 T. Domenech and S. Velankar, Capillary-driven percolating networks in ternary blends of immiscible polymers and silica particles, *Rheol. Acta*, 2014, **53**(8), 1–13.
- 14 S. S. Velankar, A non-equilibrium state diagram for liquid/fluid/particle mixtures, *Soft Matter*, 2015, **11**(43), 8393–8403.
- 15 S. J. Heidlebaugh, T. Domenech, S. V. Iasella and S. S. Velankar, Aggregation and Separation in Ternary Particle/Oil/Water Systems with Fully Wetttable Particles, *Langmuir*, 2014, **30**(1), 63–74.
- 16 S. Herminghaus, Dynamics of wet granular matter, *Adv. Phys.*, 2005, **54**(3), 221–261.
- 17 W. Pietsch, Tumble/growth agglomeration, in *Agglomeration Processes: Phenomena, Technologies, Equipment*, Wiley, Weinheim, 2008, ch. 7.
- 18 K. Boode and P. Walstra, Partial Coalescence in Oil-in-Water Emulsions 1. Nature of the Aggregation, *Colloids Surf., A*, 1993, **81**, 121–137.

- 19 M. Caggioni, A. V. Bayles, J. Lenis, E. M. Furst and P. T. Spicer, Interfacial stability and shape change of anisotropic endoskeleton droplets, *Soft Matter*, 2014, **10**(38), 7647–7652.
- 20 T. Domenech and S. S. Velankar, *J. Rheol.*, in preparation.
- 21 H. Tanaka, Viscoelastic phase separation, *J. Phys.: Condens. Matter*, 2000, **12**(15), R207–R264.
- 22 C. D. Willet, S. A. Johnson, M. J. Adams and J. P. K. Seville, Pendular capillary bridges, in *Handbook of powder technology: Granulation*, ed. A. D. Salman, M. Hounslow and J. P. K. Seville, Elsevier, Amsterdam, 2007, ch. 28, vol. 11.
- 23 X. X. Cai, B. P. Li, Y. Pan and G. Z. Wu, Morphology evolution of immiscible polymer blends as directed by nanoparticle self-agglomeration, *Polymer*, 2012, **53**(1), 259–266.
- 24 J. Khademzadeh Yeganeh, F. Goharpey, E. Moghimi, G. Petekidis and R. Foudazi, Manipulating the kinetics and mechanism of phase separation in dynamically asymmetric LCST blends by nanoparticles, *Phys. Chem. Chem. Phys.*, 2015, **17**(41), 27446–27461.
- 25 G. Wu, B. Li and J. Jiang, Carbon black self-networking induced co-continuity of immiscible polymer blends, *Polymer*, 2010, **51**(9), 2077–2083.
- 26 J. Dittmann, E. Koos and N. Willenbacher, Ceramic Capillary Suspensions: Novel Processing Route for Macroporous Ceramic Materials, *J. Am. Ceram. Soc.*, 2013, **96**(2), 391–397.
- 27 E. Koos and N. Willenbacher, Capillary Forces in Suspension Rheology, *Science*, 2011, **331**(6019), 897–900.
- 28 J. K. V. Tessmar, T. A. Holland and A. G. Mikos, Salt leaching for polymer scaffolds: laboratory-scale manufacture of cell carriers, in *Scaffolding in tissue engineering*, ed. P. X. Ma and J. Elisseeff, CRC Press, Boca Raton, 2006.
- 29 D. J. Graham and N. G. Midgley, Graphical representation of particle shape using triangular diagrams: An Excel spreadsheet method, *Earth Surf. Processes Landforms*, 2000, **25**(13), 1473–1477.